

Letter pubs.acs.org/NanoLett

# Hydrophilic, Clean Graphene for Cell Culture and Cryo-EM Imaging

Jincan Zhang,\*,<sup>\infty</sup> Kaicheng Jia, <sup>\infty</sup> Yongfeng Huang, Yanan Wang, Nan Liu, Yanan Chen, Xiaoting Liu, Xiaojun Liu, Yeshu Zhu, Liming Zheng, Heng Chen, Fushun Liang, Mengqi Zhang, Xiaojie Duan, Hongwei Wang, Li Lin,\* Hailin Peng,\* and Zhongfan Liu\*



Cite This: Nano Lett. 2021, 21, 9587-9593



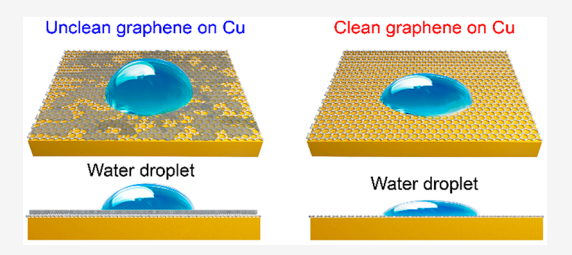
**ACCESS** 

Metrics & More

Article Recommendations

Supporting Information

ABSTRACT: The wettability of graphene is critical for numerous applications but is very sensitive to its surface cleanness. Herein, by clarifying the impact of intrinsic contamination, i.e., amorphous carbon, which is formed on the graphene surface during the high-temperature chemical vapor deposition (CVD) process, the hydrophilic nature of clean graphene grown on single-crystal Cu(111) substrate was confirmed by both experimental and theoretical studies, with an average water contact angle of  $\sim 23^{\circ}$ . Furthermore, the wettability of as-transferred graphene was proven to be highly dependent on its intrinsic cleanness, because of which the hydrophilic, clean graphene



exhibited improved performance when utilized for cell culture and cryoelectron microscopy imaging. This work not only validates the intrinsic hydrophilic nature of graphene but also provides a new insight in developing advanced bioapplications using CVDgrown clean graphene films.

KEYWORDS: Graphene, wettability, clean, hydrophilic, cell culture, cryo-EM imaging

ith its unique structure and outstanding properties, graphene has attracted intense attention in academic and industrial fields since its first isolation in 2004. Notably, great progress has been achieved in the mass production of large-area and high-quality graphene films via the chemical vapor deposition (CVD) methods, which, in turn, has enabled the rapid industrialization and commercialization of CVD graphene-based applications, such as ion sieving, biosensing, and supporting membrane for transmission electron microscopy (TEM) imaging.<sup>2–5</sup> In these applications, the interaction of graphene with water plays a crucial role, and high hydrophilicity of graphene would be highly desirable.<sup>6</sup> Therefore, controllable modification of the water wettability of graphene on functional substrates, especially the CVDgrown graphene, is of great importance for application regarding the performance and efficiency.

The static water contact angle (WCA) measurement method has been widely employed to characterize the wettability of CVD graphene film and other two-dimensional (2D) materials, such as hBN, either on growth substrates or on functional substrates, e.g., SiO<sub>2</sub>/Si, quartz, or polymer after the transfer. 9-11 Early works have pointed out the hydrophobic nature of graphene, with the measured WCA of around 90°. 12,13 Meanwhile, numerous strategies have been developed to modify the wettability of graphene via doping, 14 defect engineering, 15 or surface modification, 16,17 most of which either are time-consuming or suffer from limited compatibility with target applications. Recently, in clear contrast, several studies have presented an intrinsically hydrophilic nature of fresh graphene surface, <sup>18–20</sup> and it has been also revealed that

the wettability of graphene is very sensitive to its surroundings, especially the surface contamination, which would turn the graphene surface into a hydrophobic state. 18,19 To obtain a hydrophilic surface for practical applications, several surface cleaning methods have thus been developed to remove the contamination on graphene surface, such as airborne hydrocarbon contamination and transfer-induced polymer residues. These methods include thermal annealing,  $^{18}$  plasma etching,  $^{21,22}$  and ultraviolet— $O_3$  treatment,  $^{18,23}$  which would inevitably incur the formation of defects in the graphene lattice, resulting in degradation of graphene quality and performance.<sup>24</sup> Meanwhile, even for the hydrophilic graphene surface, the reported WCA values are still distributed in a wide range, indicating that the dominant factors for graphene wettability remain unknown. Since the wettability of graphene is very sensitive to surface contamination, the recently unveiled intrinsic contamination, i.e., amorphous carbon, which is formed on the graphene surface during the CVD growth, would also alter the surface properties of graphene. 25,26 Therefore, by removing the intrinsic contamination, it would be possible to obtain hydrophilic CVD graphene directly,

Received: August 28, 2021 Revised: October 31, 2021 Published: November 4, 2021





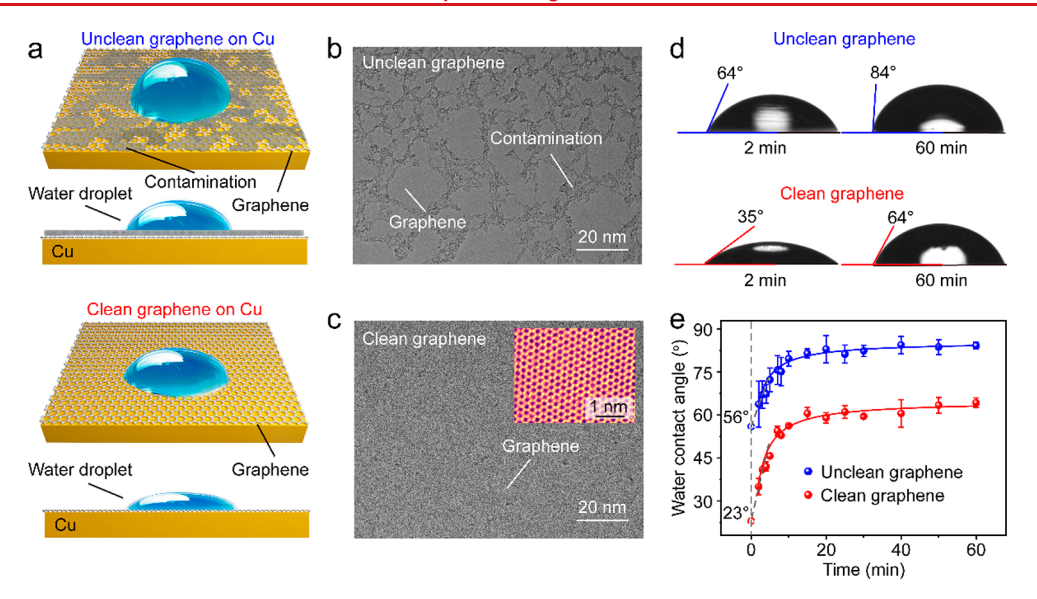


Figure 1. Wettability of CVD-derived unclean and clean graphene on Cu(111) substrates. (a) Schematic illustration of the impact of surface contamination on the wettability of graphene/Cu. (b, c) TEM images of the unclean (b) and clean (c) graphene. Inset in (c): High-resolution TEM image of the clean graphene with atomic resolution. (d) WCAs of the unclean (top) and clean (down) graphene/Cu after they were taken out of the CVD chamber for 2 min (left) and 60 min (right). (e) Time evolution of the WCAs of the Cu-supported unclean (blue) and clean (red) graphene after exposure in ambient air for 60 min.

without special treatment for practical applications, such as TEM imaging and cell culture.

In this work, the hydrophilic nature of clean graphene film on single-crystal Cu(111) substrate directly after CVD growth was confirmed, with an average WCA of  $\sim 23^{\circ}$ . The impact of amorphous carbon contamination on the graphene wettability was systematically investigated by both experimental and theoretical studies. The wettability of as-transferred graphene on quartz substrate was proven to be highly dependent on its surface cleanness; therefore, with hydrophilic surface, clean graphene exhibited improved performance when acting as the cell culture plate support. Meanwhile, the suspended clean graphene also enabled the high-density biomolecule loading for three-dimensional (3D) reconstruction when functioning as the supporting membrane for cryoelectron microscopy (cryo-EM) imaging. This work not only elucidates the intrinsic hydrophilic nature of CVD graphene but also paves new avenues for the CVD graphene-based bioapplications.

# ■ RESULTS AND DISCUSSION

The impact of the intrinsic surface contamination, i.e., amorphous carbon, on the water wettability of CVD-grown graphene on Cu was carefully investigated using static WCA measurements (Figure 1a). First, the single-crystal Cu(111) substrate, which was prepared by the epitaxial deposition of Cu on a sapphire wafer, was used as substrate for the growth of single-crystal graphene with fine flatness so that the interference from the grain boundaries of Cu and graphene, and graphene wrinkles on graphene wettability would be excluded (Figure S1a-c). The CVD growth parameters were kept the same for both clean and unclean graphene film. To obtain clean graphene surface, CO2 was introduced into the CVD chamber at 480 °C and kept for 120 min, since CO<sub>2</sub> can selectively etch away amorphous carbon without producing new defects.<sup>27</sup> After the CO<sub>2</sub> treatment, a polymer-free transfer method<sup>28</sup> was employed to transfer the graphene film onto commercial holey carbon TEM grids for evaluating the cleanness (Figure S2). As shown in Figure 1b, for conventionally grown graphene, the amorphous carbon contamination (dark contrast) almost occupied about 40% of the area, and continuous clean regions were no larger than 100 nm in size. In contrast, graphene was observed with a uniform and brighter contrast in the TEM image after the  $\rm CO_2$  treatment (Figure 1c), indicating that surface contamination on graphene surface had been largely etched away by the  $\rm CO_2$ . Meanwhile, a clear graphene lattice without any defects was observed in the atomically resolved TEM image (Figure 1c, inset), confirming no defects produced in  $\rm CO_2$  treatment. This was also evidenced by the D band-free Raman spectra of the graphene after the transfer (Figure S1d-f).

Water droplets of ~4 µL were deposited on the graphene/ Cu surfaces to perform static WCA measurements. To avoid the airborne hydrocarbon contamination, 29-31 the WCA measurements were conducted directly after the growth. As shown in Figure 1d, the clean graphene exhibited a hydrophilic nature with an average WCA of ~35°, while the unclean graphene exhibited an average WCA of ~64°. Temporal evolution of the WCA on the graphene/Cu samples after being taken out the growth chamber was carefully measured to further understand the influence of absorbed airborne contamination on graphene wettability (Figures S3 and S4). As shown in Figure 1e, the WCAs of both the clean and unclean graphene increased sharply within the first 10 min after being taken out from the growth chamber. Subsequently, WCA values increased slowly after 20 min exposure and gradually reached the maximum value. Moreover, the initial WCAs of the clean and unclean graphene can be estimated by extending the measured lines in Figure 1e with obtained slopes as the increase rate of WCA values was nearly constant in the initial stage. Therefore, estimated initial WCAs of clean and unclean graphene are  $\sim 23^{\circ}$  and  $\sim 56^{\circ}$ , respectively. It should be noted that the difference of WCAs between clean and unclean graphene lasted at least 60 min, which shows potential for large-area evaluation of the surface cleanness of CVD graphene by water visualization in a nondestructive manner (Figure S5). In addition, the parameters utilized in CO<sub>2</sub>

Nano Letters pubs.acs.org/NanoLett Letter

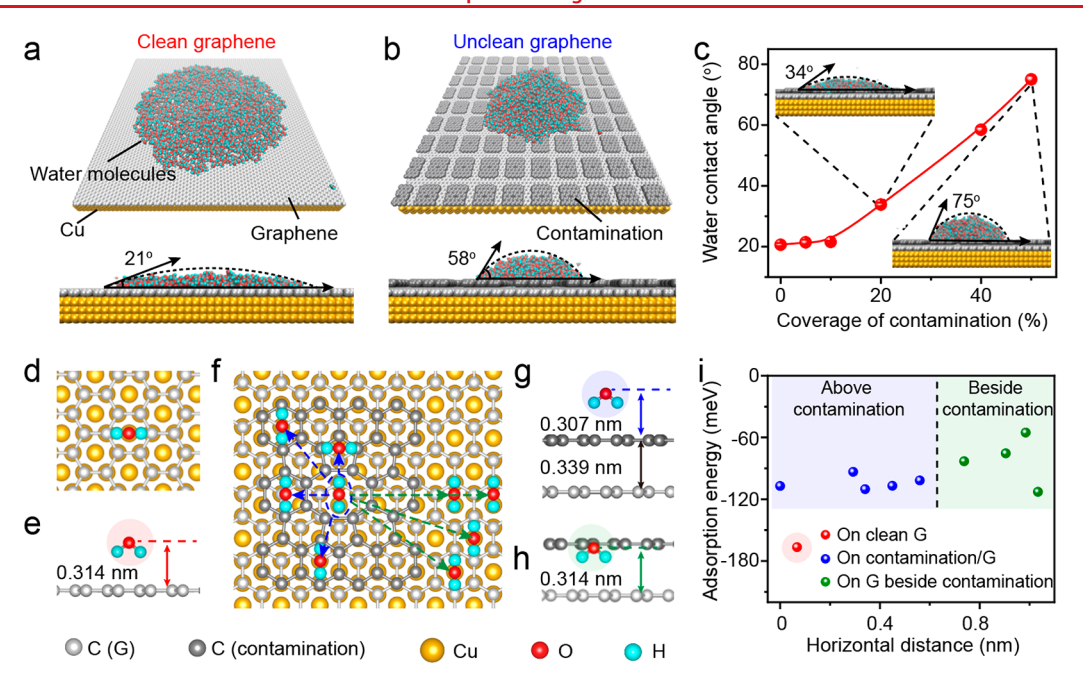


Figure 2. Theoretical analysis of the water wettability on graphene/Cu. (a, b) Representative MD simulation results of the water molecules distribution on the clean (a) and unclean (b) (with contamination coverage of 40%) graphene/Cu(111) surface. (c) Relationship between the WCA values of graphene and the coverage of surface contamination. Inset: MD simulation results of the unclean graphene with the contamination coverage of 20% (up left) and 50% (bottom right). (d, e) Top (d) and side (e) views of the water molecule adsorbed atop clean graphene surface. (f) Top view of the water molecules adsorbed on the surface of the contaminated graphene with varied horizontal distance. (g, h) Representative side views of the water molecule adsorbed above the contamination (g) and above graphene beside the contamination (h). (i) Relationship between the adsorption energy of the water molecules and the horizontal distance from O atom in the water molecule to the center of the amorphous carbon contamination.

treatment of graphene surface also affect the wettability of graphene (Figure S6).

Molecular dynamic (MD) and density functional theory (DFT) simulations were performed to investigate the wetting behavior of water on graphene surface (Figures S7 and S8). Note that the 5-8-5 topological defect, one of the commonly observed defects in graphene, 27,32 was used as the simplified model to represent the amorphous carbon contamination to investigate the impact of surface contamination on the wettability of graphene (Figure S7c,d and Figure S8b,c). In the MD simulations, thousands of water molecules were put on the top surface of graphene, and after 4 ns equilibrium, the WCA was obtained by fitting the hemisphere-shaped water droplet using the Young equation. The clean graphene/ Cu(111) was calculated to have a WCA of  $\sim 21^{\circ}$  (Figure 2a), consistent with the experimental observation. The presence of surface contamination on the graphene/Cu surface would cause an increase of WCA to ~58° (Figure 2b), leaving the unclean graphene less hydrophilic. Furthermore, as the ratio of contaminated area increased from 0% to 50%, the calculated WCA values would increase from  $\sim 21^{\circ}$  to  $\sim 75^{\circ}$  (Figure 2c).

DFT simulations were further performed to clarify the interactions between water and graphene by calculating the adsorption energy of the water molecule on graphene, since water adsorption energy was reported to be related to the graphene wettability.<sup>33,34</sup> By finding the minimum ground state energy of the water molecule adsorbed on the clean graphene/Cu(111) surface, the most stable adsorption configuration of water molecules can be confirmed (Figure 2d,e and Figure S9a,b), in which the distance between the oxygen atom of water molecule and the graphene plane (that is, height of the water molecule) was 0.314 nm with adsorption energy of

-166.95 meV. In the meantime, the stable configuration of water molecule on unclean graphene/Cu(111) surface was 0.307 nm higher than the contaminated graphene plane (Figure S9c,d), with an adsorption energy of -107.15 meV.

Subsequently, the adsorption energies of water molecules on four other sites atop the contamination were calculated by varying the horizontal distances for water molecules to the center of the amorphous carbon contamination, and the obtained adsorption energy ranged from -110 meV to -93 meV (Figure 2f,g). Since that the unclean graphene surface is partly covered by the amorphous carbon contamination, we also investigated the adsorption behavior of the water molecules on the graphene regions surrounded by contamination (Figure 2h and Figure S9e,f). These water molecules exhibited an adsorption energy ranging from -113 to -55 meV, when horizontal distances from water molecules to the center of the contaminated region varied from 0.74 to 1.03 nm (Figure 2i). Generally, a smaller adsorption energy indicates a stronger interaction between water and graphene and therefore a more hydrophilic surface.<sup>34</sup> Therefore, a larger adsorption energy of water molecules on the unclean graphene confirmed the less hydrophilic behaviors of the contaminated graphene.

After CVD growth, the transfer of graphene onto other functional substrates is required for practical applications.<sup>35</sup> To transfer graphene onto quartz substrates, which are commonly used for cell culture,<sup>36</sup> polymethyl methacrylate (PMMA) was employed as the transfer medium to support graphene films during the transfer process.<sup>25</sup> Owing to the stronger interaction between PMMA and amorphous carbon with abundant dangling bonds, PMMA residues would be easily left on the unclean graphene surface after the transfer, while a much cleaner surface can be obtained when transferring clean

Nano Letters pubs.acs.org/NanoLett Letter

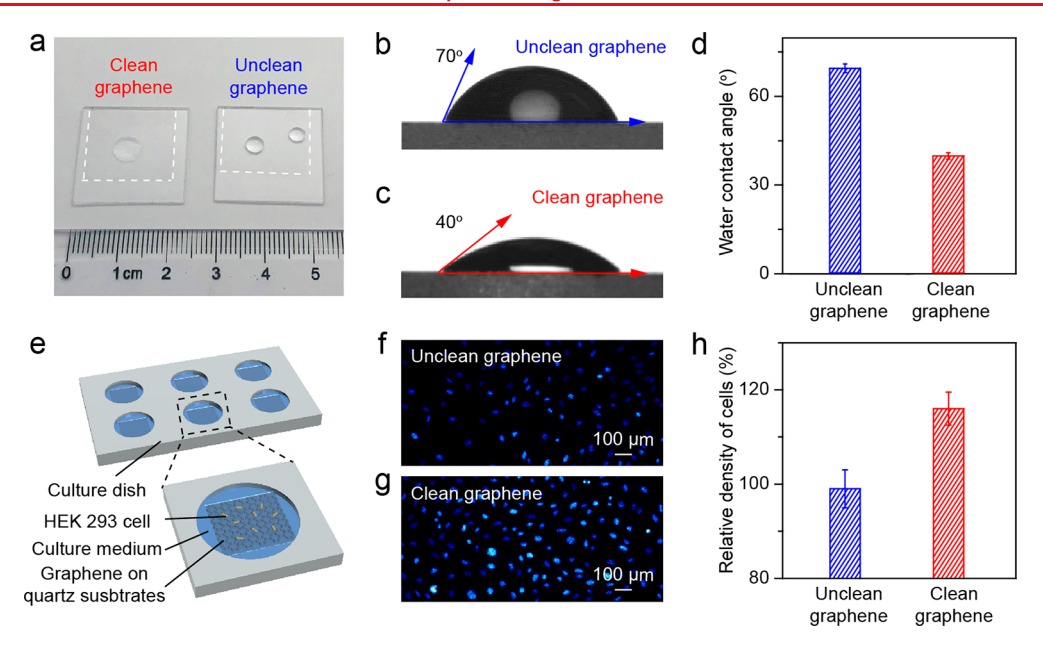


Figure 3. Application of the clean graphene in cell culture. (a) Photograph of water droplets on the clean (left) and unclean (right) graphene supported by the quartz substrates. (b, c) WCA measurement results of the as-transferred unclean (b) and clean (c) graphene on quartz substrates. (d) Statistical results of the WCA values of the unclean (blue) and clean (red) graphene on quartz substrates. (e) Schematic illustration of the cell culture using graphene as the culture plate support. (f, g) Fluorescence microscope images of cultured cells on the unclean (f) and clean (g) graphene surface after proliferation for 48 h. (h) Comparison of the density of cells cultured on the unclean (blue) and clean (red) graphene on quartz substrates, using the cell density on the bare quartz substrate as a reference.

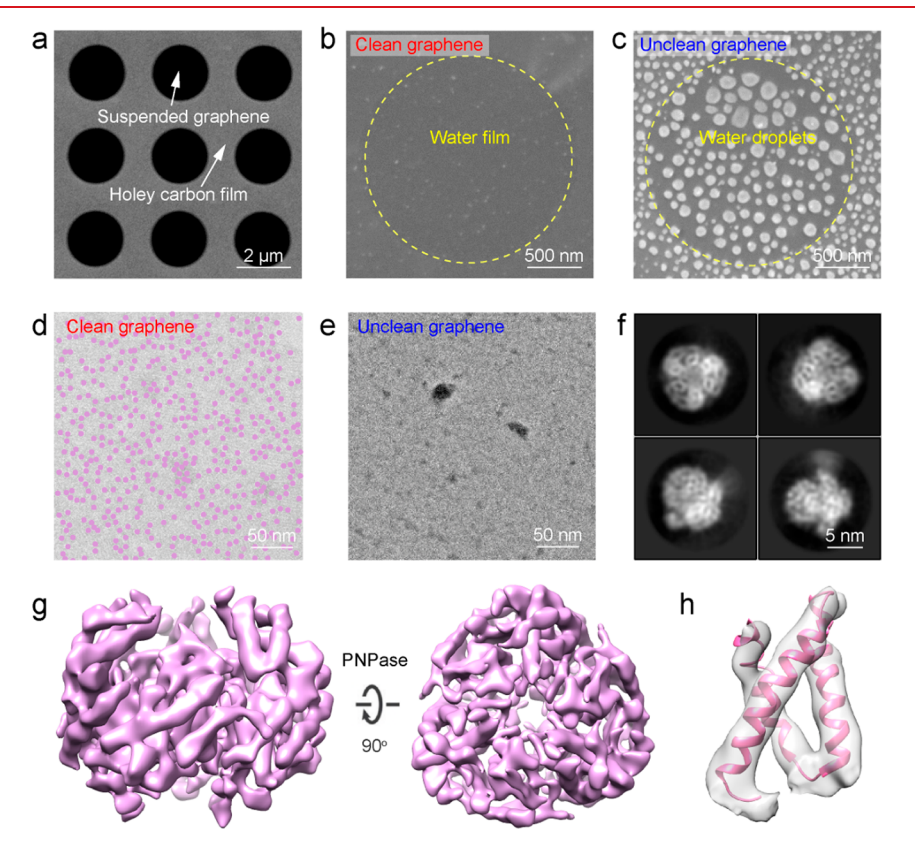


Figure 4. Application of the clean graphene on cryo-EM imaging. (a) Scanning EM (SEM) image of the large-area suspended graphene membrane. (b, c) SEM images showing the distribution of water on the surface of the suspended clean (b) and unclean (c) graphene. (d, e) TEM images showing the distribution of ice layer and PNPase particles on the clean (d) and unclean (e) graphene. Note that PNPase particles are dyed in semitransparent purple color in (d). (f) Representative 2D class averages of PNPase supported by the clean graphene. (g) 3D reconstruction map of the PNPase particle using the clean graphene as the supporting substrate. (h) Selected region of PNPase's map with the corresponding model docked. 42

graphene (Figure S10). Due to the different amount of surface contamination, the cm-sized as-transferred clean and unclean graphene samples exhibited a clear difference of wettability (Figure 3a). The average WCA is  $\sim 40^{\circ}$  and  $\sim 70^{\circ}$  for clean and unclean graphene (Figure 3b–d), respectively, suggesting that after transfer, the hydrophilic nature of clean graphene is retained.

The clean graphene and unclean graphene on quartz substrates were next both employed as the plate support for cell culture (Figure 3e) to evaluate the biocompatibility of the transferred graphene and the impact of its surface cleanness and wettability on the cell proliferation rate. The HEK 293 cell was selected for the cell proliferation experiment, and the culture time was set as 48 h. The number of cultured cells was then counted and carefully compared based on the fluorescent images of the cultured cells, which were acquired with the aid of Hoechst staining technology. The number of cells cultured on the clean graphene was higher than that on the unclean graphene surface (Figure 3f,g), which can be attributed to the improved wettability and the higher surface flatness, indicative of the better biocompatibility of the clean graphene. 37-39 The statistical result of cell density further confirmed the increased cell proliferation rate on the clean graphene in comparison with the unclean graphene and bare quartz substrate (Figure 3h and Figure S11). The above experiment proves the potential of clean graphene as the biological labware for cell biology investigation.

The clean graphene film with promising hydrophilicity would also have potential for the applications in cryo-EM imaging by enabling the formation of uniform thin ice layers and minimization of the background signal, where graphene would function as the supporting film. 16,22,40 To evaluate the impact of surface contamination on the spatial distribution of water on graphene surfaces, cryoenvironmental scanning EM (ESEM) and cryo-TEM characterizations were conducted on the suspended graphene membrane (Figure 4a and Figure S12a). Before the cryo-ESEM imaging, the suspended graphene samples were first exposed to stable water vapors for 10 s and then immediately put into the liquid nitrogen to prepare the vitrified cryosamples. This process was carefully optimized in order to minimize the phase change of water during cooling. The high-magnification ESEM images in the region of single hole revealed a marked difference in the water distribution on the unclean and clean graphene surfaces. A continuous water membrane with uniform contrast was formed on the clean graphene surface (Figure 4b and Figure S12b) while high-density spherical-shaped water droplets were observed on the surface of unclean graphene (Figure 4c), demonstrating better wettability of clean graphene.

We further revealed the impact of surface cleanness of graphene on its interaction with biomolecules by applying the graphene grids for preparing cryospecimens of PNPase protein and characterizing them by cryo-TEM. To minimize the additional impact of airborne contamination, the unclean and clean graphene grids were both sealed in glass containers and stored in dry ice before being applied for the specimen preparation for TEM imaging.<sup>41</sup> Note that the initial cleanness and wettability of the graphene would determine the uniformity of the ice layers and the distribution of the PNPase particles. Specifically, a dense and uniform distribution of PNPase particles in the uniform ice layer was clearly observed on the clean graphene surface (Figure 4d and Figure S12c), while few PNPase particles were observed on the unclean

graphene surface, consistent with previously reported results using conventional graphene growth and transfer method (Figure 4e). Therefore, on the basis of the statistic of the particle density on the clean and unclean graphene samples (Figure S12d), we can conclude that the high surface cleanness of graphene is crucial for cryo-EM analysis of biomolecules. Notably, PNPase particles adopted rich orientations on the suspended clean graphene membrane (Figure 4f), enabling a reliable 3D cryo-EM reconstruction of PNPase, with the secondary structural information nicely identified (Figure 4g,h and Figure S13).

# CONCLUSION

This study demonstrates the hydrophilic nature of clean graphene and clarifies the impact of intrinsic contamination on graphene wettability by both experimental and theoretical studies. Furthermore, after being transferred onto functional substrates, the clean graphene remains more hydrophilic than its unclean counterpart and thus exhibites obvious advantages for the applications in cell culture and cryo-EM imaging. This work not only validates the intrinsic hydrophilic nature of graphene but also provides a new insight in developing advanced applications based on CVD graphene with a clean surface.

## ASSOCIATED CONTENT

# Supporting Information

The Supporting Information is available free of charge at https://pubs.acs.org/doi/10.1021/acs.nanolett.1c03344.

Methods, characterization information, and additional figures as described in the text (PDF)

# AUTHOR INFORMATION

# **Corresponding Authors**

Jincan Zhang — Center for Nanochemistry, Beijing Science and Engineering Center for Nanocarbons, Beijing National Laboratory for Molecular Science, College of Chemistry and Molecular Engineering and Academy for Advanced Interdisciplinary Studies, Peking University, Beijing 100871, P. R. China; Beijing Graphene Institute, Beijing 100095, P. R. China; Department of Engineering, University of Cambridge, Cambridge CB3 0FA, U.K.; Email: zhangjc-cnc@pku.edu.cn

Li Lin — Materials Science and Engineering, National University of Singapore, 119077, Singapore; Email: linlicnc@pku.edu.cn

Hailin Peng — Center for Nanochemistry, Beijing Science and Engineering Center for Nanocarbons, Beijing National Laboratory for Molecular Science, College of Chemistry and Molecular Engineering, Peking University, Beijing 100871, P. R. China; Beijing Graphene Institute, Beijing 100095, P. R. China; orcid.org/0000-0003-1569-0238; Email: hlpeng@pku.edu.cn

Zhongfan Liu — Center for Nanochemistry, Beijing Science and Engineering Center for Nanocarbons, Beijing National Laboratory for Molecular Science, College of Chemistry and Molecular Engineering, Peking University, Beijing 100871, P. R. China; Beijing Graphene Institute, Beijing 100095, P. R. China; orcid.org/0000-0003-0065-7988; Email: zfliu@pku.edu.cn

Nano Letters pubs.acs.org/NanoLett Letter

#### **Authors**

- Kaicheng Jia Center for Nanochemistry, Beijing Science and Engineering Center for Nanocarbons, Beijing National Laboratory for Molecular Science, College of Chemistry and Molecular Engineering, Peking University, Beijing 100871, P. R. China; Beijing Graphene Institute, Beijing 100095, P. R. China
- Yongfeng Huang Songshan Lake Materials Laboratory, Dongguan, Guangdong 523808, P. R. China; Beijing National Laboratory for Condensed Matter Physics and Institute of Physics, Chinese Academy of Sciences, Beijing 100190, P. R. China
- Yanan Wang Songshan Lake Materials Laboratory, Dongguan, Guangdong 523808, P. R. China; Beijing National Laboratory for Condensed Matter Physics and Institute of Physics, Chinese Academy of Sciences, Beijing 100190, P. R. China
- Nan Liu Ministry of Education Key Laboratory of Protein Sciences, Beijing Advanced Innovation Center for Structural Biology, School of Life Sciences and Tsinghua-Peking Joint Center for Life Sciences, Tsinghua University, Beijing 100084, P. R. China
- Yanan Chen Ministry of Education Key Laboratory of Protein Sciences, Beijing Advanced Innovation Center for Structural Biology, School of Life Sciences and Tsinghua-Peking Joint Center for Life Sciences, Tsinghua University, Beijing 100084, P. R. China
- Xiaoting Liu Center for Nanochemistry, Beijing Science and Engineering Center for Nanocarbons, Beijing National Laboratory for Molecular Science, College of Chemistry and Molecular Engineering and Academy for Advanced Interdisciplinary Studies, Peking University, Beijing 100871, P. R. China; Beijing Graphene Institute, Beijing 100095, P. R. China
- Xiaojun Liu College of Future Technology, Peking University, Beijing 100871, P. R. China
- Yeshu Zhu Center for Nanochemistry, Beijing Science and Engineering Center for Nanocarbons, Beijing National Laboratory for Molecular Science, College of Chemistry and Molecular Engineering and Academy for Advanced Interdisciplinary Studies, Peking University, Beijing 100871, P. R. China; Beijing Graphene Institute, Beijing 100095, P. R. China
- Liming Zheng Center for Nanochemistry, Beijing Science and Engineering Center for Nanocarbons, Beijing National Laboratory for Molecular Science, College of Chemistry and Molecular Engineering, Peking University, Beijing 100871, P. R. China; Beijing Graphene Institute, Beijing 100095, P. R. China
- Heng Chen Center for Nanochemistry, Beijing Science and Engineering Center for Nanocarbons, Beijing National Laboratory for Molecular Science, College of Chemistry and Molecular Engineering, Peking University, Beijing 100871, P. R. China; Beijing Graphene Institute, Beijing 100095, P. R. China
- Fushun Liang Center for Nanochemistry, Beijing Science and Engineering Center for Nanocarbons, Beijing National Laboratory for Molecular Science, College of Chemistry and Molecular Engineering and Academy for Advanced Interdisciplinary Studies, Peking University, Beijing 100871, P. R. China; Beijing Graphene Institute, Beijing 100095, P. R. China

- Mengqi Zhang Beijing Graphene Institute, Beijing 100095, P. R. China
- Xiaojie Duan College of Future Technology, Peking University, Beijing 100871, P. R. China; orcid.org/0000-0001-7799-3897
- Hongwei Wang Ministry of Education Key Laboratory of Protein Sciences, Beijing Advanced Innovation Center for Structural Biology, School of Life Sciences and Tsinghua-Peking Joint Center for Life Sciences, Tsinghua University, Beijing 100084, P. R. China; orcid.org/0000-0001-9494-8780

Complete contact information is available at: https://pubs.acs.org/10.1021/acs.nanolett.1c03344

#### **Author Contributions**

 $^{\infty}$ J.Z. and K.J. contributed equally. The manuscript was written through contributions of all authors. All authors have given approval to the final version of the manuscript.

#### Notes

The authors declare no competing financial interest.

▲ School of Materials Science and Engineering, Peking University, Beijing 100871, P. R. China

#### ACKNOWLEDGMENTS

The authors thank Beijing National Laboratory for Molecular Sciences (Grant BNLMS-CXTD-202001). This work was financially supported by National Basic Research Program of China (Grants 2016YFA0200101 and 2018YFA0703502), National Natural Science Foundation of China (Grants 21525310, 51520105003, 52072042, and 11904389), Beijing Municipal Science & Technology Commission (Grants Z181100004818001, Z18110300480001, Z18110300480002, Z191100000819005, and Z201100008720005), China Postdoctoral Science Foundation (Grant 2019TQ0347), and GuangDong Basic and Applied Basic Research Foundation (Grant 2020A1515110743). We thank the computational resources of Platform for Data-Driven Computational Materials Discovery at the Songshan Lake Materials Laboratory in Dongguan, and Center for Quantum Simulation Sciences at the Institute of Physics. We also acknowledge the Electron Microscopy Laboratory in Peking University for the use of their electron microscopes.

# **■** REFERENCES

- (1) Ye, R.; Tour, J. M. Graphene at fifteen. ACS Nano 2019, 13 (10), 10872-10878.
- (2) Kong, W.; Kum, H.; Bae, S. H.; Shim, J.; Kim, H.; Kong, L.; Meng, Y.; Wang, K.; Kim, C.; Kim, J. Path towards graphene commercialization from lab to market. *Nat. Nanotechnol.* **2019**, *14* (10), 927–938.
- (3) Lin, L.; Peng, H. L.; Liu, Z. F. Synthesis challenges for graphene industry. *Nat. Mater.* **2019**, *18* (6), 520–524.
- (4) Zhou, K. G.; Vasu, K. S.; Cherian, C. T.; Neek-Amal, M.; Zhang, J. C.; Ghorbanfekr-Kalashami, H.; Huang, K.; Marshall, O. P.; Kravets, V. G.; Abraham, J.; Su, Y.; Grigorenko, A. N.; Pratt, A.; Geim, A. K.; Peeters, F. M.; Novoselov, K. S.; Nair, R. R. Electrically controlled water permeation through graphene oxide membranes. *Nature* **2018**, *559* (7713), 236–240.
- (5) Keerthi, A.; Geim, A. K.; Janardanan, A.; Rooney, A. P.; Esfandiar, A.; Hu, S.; Dar, S. A.; Grigorieva, I. V.; Haigh, S. J.; Wang, F. C.; Radha, B. Ballistic molecular transport through two-dimensional channels. *Nature* **2018**, *558* (7710), 420–424.

- (6) Feng, J.; Guo, Z. Wettability of graphene: from influencing factors and reversible conversions to potential applications. *Nanoscale Horiz.* **2019**, 4 (2), 339–364.
- (7) Snapp, P.; Kim, J. M.; Cho, C.; Leem, J.; Haque, M. F.; Nam, S. Interaction of 2D materials with liquids: wettability, electrochemical properties, friction, and emerging directions. *NPG Asia Mater.* **2020**, 12 (1), 22.
- (8) Wang, J.; Gao, W.; Zhang, H.; Zou, M. H.; Chen, Y. P.; Zhao, Y. J. Programmable wettability on photocontrolled graphene film. *Sci. Adv.* **2018**, *4* (9), eaat7392.
- (9) Melios, C.; Giusca, C. E.; Panchal, V.; Kazakova, O. Water on graphene: review of recent progress. 2D Mater. 2018, 5 (2), 022001.
- (10) Belyaeva, L. A.; Schneider, G. F. Wettability of graphene. Surf. Sci. Rep. 2020, 75 (2), 100482.
- (11) Li, X.; Qiu, H.; Liu, X.; Yin, J.; Guo, W. Wettability of supported monolayer hexagonal boron nitride in air. *Adv. Funct. Mater.* **2017**, 27 (19), 1603181.
- (12) Raj, R.; Maroo, S. C.; Wang, E. N. Wettability of graphene. *Nano Lett.* **2013**, *13* (4), 1509–1515.
- (13) Hong, G.; Han, Y.; Schutzius, T. M.; Wang, Y.; Pan, Y.; Hu, M.; Jie, J.; Sharma, C. S.; Muller, U.; Poulikakos, D. On the Mechanism of hydrophilicity of graphene. *Nano Lett.* **2016**, *16* (7), 4447–4453.
- (14) Ashraf, A.; Wu, Y. B.; Wang, M. C.; Yong, K.; Sun, T.; Jing, Y. H.; Haasch, R. T.; Aluru, N. R.; Nam, S. Doping-Induced tunable wettability and adhesion of graphene. *Nano Lett.* **2016**, *16* (8), 5318–5318
- (15) Kozbial, A.; Trouba, C.; Liu, H.; Li, L. Characterization of the intrinsic water wettability of graphite using contact angle measurements: effect of defects on static and dynamic contact angles. *Langmuir* **2017**, 33 (4), 959–967.
- (16) Liu, N.; Zhang, J.; Chen, Y.; Liu, C.; Zhang, X.; Xu, K.; Wen, J.; Luo, Z.; Chen, S.; Gao, P.; Jia, K.; Liu, Z.; Peng, H.; Wang, H. W. Bioactive functionalized monolayer graphene for high-resolution Cryo-Electron microscopy. *J. Am. Chem. Soc.* **2019**, *141* (9), 4016–4025.
- (17) Son, J.; Lee, J. Y.; Han, N.; Cha, J.; Choi, J.; Kwon, J.; Nam, S.; Yoo, K. H.; Lee, G. H.; Hong, J. Tunable wettability of graphene through nondestructive hydrogenation and wettability-based patterning for bioapplications. *Nano Lett.* **2020**, *20* (8), 5625–5631.
- (18) Li, Z.; Wang, Y.; Kozbial, A.; Shenoy, G.; Zhou, F.; McGinley, R.; Ireland, P.; Morganstein, B.; Kunkel, A.; Surwade, S. P.; Li, L.; Liu, H. Effect of airborne contaminants on the wettability of supported graphene and graphite. *Nat. Mater.* **2013**, *12* (10), 925–931.
- (19) Prydatko, A. V.; Belyaeva, L. A.; Jiang, L.; Lima, L. M. C.; Schneider, G. F. Contact angle measurement of free-standing square-millimeter single-layer graphene. *Nat. Commun.* **2018**, *9* (1), 4185.
- (20) Belyaeva, L. A.; van Deursen, P. M. G.; Barbetsea, K. I.; Schneider, G. F. Hydrophilicity of graphene in water through transparency to polar and dispersive interactions. *Adv. Mater.* **2018**, 30 (6), 1703274.
- (21) Zheng, L. M.; Chen, Y. N.; Li, N.; Zhang, J. C.; Liu, N.; Liu, J. J.; Dang, W. H.; Deng, B.; Li, Y. B.; Gao, X. Y.; Tan, C. W.; Yang, Z.; Xu, S. P.; Wang, M. Z.; Yang, H.; Sun, L. Z.; Cui, Y.; Wei, X. D.; Gao, P.; Wang, H. W.; Peng, H. L. Robust ultraclean atomically thin membranes for atomic-resolution electron microscopy. *Nat. Commun.* 2020, 11 (1), 541.
- (22) Russo, C. J.; Passmore, L. A. Controlling protein adsorption on graphene for cryo-EM using low-energy hydrogen plasmas. *Nat. Methods* **2014**, *11* (7), 773–773.
- (23) Xu, Z.; Ao, Z.; Chu, D.; Younis, A.; Li, C. M.; Li, S. Reversible hydrophobic to hydrophilic transition in graphene via water splitting induced by UV irradiation. *Sci. Rep.* **2015**, *4*, 6450.
- (24) Zheng, L.; Chen, Y.; Li, N.; Zhang, J.; Liu, N.; Liu, J.; Dang, W.; Deng, B.; Li, Y.; Gao, X.; Tan, C.; Yang, Z.; Xu, S.; Wang, M.; Yang, H.; Sun, L.; Cui, Y.; Wei, X.; Gao, P.; Wang, H. W.; Peng, H. Robust ultraclean atomically thin membranes for atomic-resolution electron microscopy. *Nat. Commun.* 2020, 11 (1), 541.

- (25) Zhang, J.; Sun, L.; Jia, K.; Liu, X.; Cheng, T.; Peng, H.; Lin, L.; Liu, Z. New growth frontier: superclean graphene. ACS Nano 2020, 14 (9), 10796–10803.
- (26) Lin, L.; Zhang, J.; Su, H.; Li, J.; Sun, L.; Wang, Z.; Xu, F.; Liu, C.; Lopatin, S.; Zhu, Y.; Jia, K.; Chen, S.; Rui, D.; Sun, J.; Xue, R.; Gao, P.; Kang, N.; Han, Y.; Xu, H. Q.; Cao, Y.; Novoselov, K. S.; Tian, Z.; Ren, B.; Peng, H.; Liu, Z. Towards super-clean graphene. *Nat. Commun.* **2019**, *10* (1), 1912.
- (27) Zhang, J.; Jia, K.; Lin, L.; Zhao, W.; Quang, H. T.; Sun, L.; Li, T.; Li, Z.; Liu, X.; Zheng, L.; Xue, R.; Gao, J.; Luo, Z.; Rummeli, M. H.; Yuan, Q.; Peng, H.; Liu, Z. Large-area synthesis of superclean graphene via selective etching of amorphous carbon with carbon dioxide. *Angew. Chem., Int. Ed.* **2019**, *58* (41), 14446–14451.
- (28) Zhang, J.; Lin, L.; Sun, L.; Huang, Y.; Koh, A. L.; Dang, W.; Yin, J.; Wang, M.; Tan, C.; Li, T.; Tan, Z.; Liu, Z.; Peng, H. Clean transfer of large graphene single crystals for high-intactness suspended membranes and liquid cells. *Adv. Mater.* **2017**, 29 (26), 1700639.
- (29) Kozbial, A.; Zhou, F.; Li, Z.; Liu, H.; Li, L. Are graphitic surfaces hydrophobic? *Acc. Chem. Res.* **2016**, 49 (12), 2765–2773.
- (30) Aria, A. I.; Kidambi, P. R.; Weatherup, R. S.; Xiao, L.; Williams, J. A.; Hofmann, S. Time evolution of the wettability of supported graphene under ambient air exposure. *J. Phys. Chem. C* **2016**, *120* (4), 2215–2224.
- (31) Amadei, C. A.; Lai, C. Y.; Heskes, D.; Chiesa, M. Time dependent wettability of graphite upon ambient exposure: the role of water adsorption. *J. Chem. Phys.* **2014**, *141* (8), 084709.
- (32) Banhart, F.; Kotakoski, J.; Krasheninnikov, A. V. Structural defects in graphene. *ACS Nano* **2011**, *5* (1), 26–41.
- (33) Ma, J.; Michaelides, A.; Alfè, D.; Schimka, L.; Kresse, G.; Wang, E. Adsorption and diffusion of water on graphene from first principles. *Phys. Rev. B: Condens. Matter Mater. Phys.* **2011**, 84 (3), 033402.
- (34) Werder, T.; Walther, J. H.; Jaffe, R.; Halicioglu, T.; Koumoutsakos, P. On the water–carbon interaction for use in molecular dynamics simulations of graphite and carbon nanotubes. *J. Phys. Chem. B* **2003**, *107* (6), 1345–1352.
- (35) Song, Y.; Zou, W.; Lu, Q.; Lin, L.; Liu, Z. Graphene transfer: paving the road for applications of chemical vapor deposition graphene. *Small* **2021**, 2007600.
- (36) Chen, Y.; Sun, J.; Gao, J.; Du, F.; Han, Q.; Nie, Y.; Chen, Z.; Bachmatiuk, A.; Priydarshi, M. K.; Ma, D.; Song, X.; Wu, X.; Xiong, C.; Rummeli, M. H.; Ding, F.; Zhang, Y.; Liu, Z. Growing uniform graphene disks and films on molten glass for heating devices and cell culture. *Adv. Mater.* **2015**, 27 (47), 7839–7846.
- (37) Liu, X.; Lim, J. Y.; Donahue, H. J.; Dhurjati, R.; Mastro, A. M.; Vogler, E. A. Influence of substratum surface chemistry/energy and topography on the human fetal osteoblastic cell line hFOB 1.19: Phenotypic and genotypic responses observed in vitro. *Biomaterials* **2007**, 28 (31), 4535–4550.
- (38) Lim, J. Y.; Loiselle, A. E.; Lee, J. S.; Zhang, Y.; Salvi, J. D.; Donahue, H. J. Optimizing the osteogenic potential of adult stem cells for skeletal regeneration. *J. Orthop. Res.* **2011**, 29 (11), 1627–1633.
- (39) Lim, J. Y.; Shaughnessy, M. C.; Zhou, Z.; Noh, H.; Vogler, E. A.; Donahue, H. J. Surface energy effects on osteoblast spatial growth and mineralization. *Biomaterials* **2008**, *29* (12), 1776–1784.
- (40) Kato, R.; Hatano, Y.; Kasahata, N.; Sato, C.; Suenaga, K.; Hasegawa, M. High-precision thickness control of ice layer on CVD grown bilayer graphene for cryo-TEM. *Carbon* **2020**, *160*, 107–112.
- (41) Li, Z.; Kozbial, A.; Nioradze, N.; Parobek, D.; Shenoy, G. J.; Salim, M.; Amemiya, S.; Li, L.; Liu, H. Water protects graphitic surface from airborne hydrocarbon contamination. *ACS Nano* **2016**, *10* (1), 349–359.
- (42) Shi, Z.; Yang, W.-Z.; Lin-Chao, S.; Chak, K.-F.; Yuan, H. S. Crystal structure of Escherichia coli PNPase: Central channel residues are involved in processive RNA degradation. RNA 2008, 14 (11), 2361–2371.